

Analysis of vertical and horizontal flows of liquids and gases through a wire-mesh sensor

Abstract. W artykule przedstawiono analizę pionowych i poziomych przepływów cieczy i gazów przez czujnik z siatki drucianej. Rozwiązanie nie wymaga skomplikowanej rekonstrukcji programu, która charakteryzuje się bardzo dużą prędkością działania w zależności od zastosowanego konwertera analogowo-cyfrowego. Czujnik składa się z dwóch części: modułu akwizycji i części roboczej. Urządzenie umożliwia badanie przepływów wielofazowych oraz klasyczne badanie pęcherzyków powietrza. Przewody jednej płaszczyzny są używane jako nadajniki, a przewody drugiej płaszczyzny jako odbiorniki. Próbki ze wszystkich linii odbiorczych są pobierane w tym samym czasie.

Streszczenie. The article presents the analysis of vertical and horizontal flows of liquids and gases through a wire mesh sensor. The solution does not require complicated reconstruction of the program, which is characterized by a very high speed of operation depending on the analog-to-digital converter used. The sensor consists of two parts: the acquisition module and the working part. The device allows testing of multiphase flows and classic air bubble testing. The wires of one plane are used as transmitters, and the wires of the other plane as receivers. Samples from all receiving lines are taken at the same time. (*Analiza pionowych i poziomych przepływów cieczy i gazów przez czujnik siatkowy*).

Keywords: wire-mesh sensor, two-phase flow.

Słowa kluczowe: sensor siatkowy, przepływ dwufazowy.

Introduction

Wire-mesh sensor is a device for invasive imaging of vertical and horizontal flows of liquids and gases [1,2,4]. It does not require any complicated software reconstruction, which is why it is characterized by very high operating speed, which depends to the greatest extent on the conversion time of the analog-to-digital converter used. The sensor consists of two parts: the acquisition module and the working part [4] [5]. The device allows testing of multiphase flows and classic testing of air bubbles that are usually performed in air-lift reactors [9]. Sensors are also suitable for testing various types of surface flows and movement of bulk materials along the bottom of a pipeline due to their high time resolution [2] [3,7,8]. The price for very high efficiency is, of course, invasiveness, but research shows the level of uncertainty of measuring these devices oscillating around 10% [6].

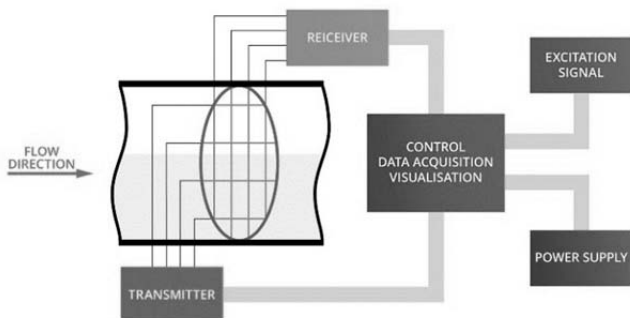


Fig. 1. WMS block diagram.

There are several types of WMS that differ in their mode of operation or design, among which the most important can be listed:

- impedance (also called conductance) - using voltage measurement between transmission and measuring lines (used in the described project),
- capacitive [2,5,10] - using the measurement of capacitance between transmission and measuring lines, enables measurements of non-conductive media,

- thermal [7] - using thermistors connecting transmission and reception lines,
- three-plane - having an additional plane of receiving lines.

The method of operation of the device (regardless of its design) comes down to transmitting signals on the transmission lines and measuring these signals on the receiving lines. Transmission and measurements take place in a specific sequence - for each individually activated transmission line there are measurements on all receiving lines. After completing a single cycle of all beats and the measurements assigned to them, the control system has numerical data about one frame of the image. It can immediately show it on the display, no image reconstruction is required. The specific value of the tested size (voltage, capacity) is assigned a specific pixel color as each pixel is in fact the point of intersection of one transmission line with one receiving line. The WMS sensor data acquisition speed depends on the transducer used, the microprocessor system controlling the entire device, the working time of the keys, decoders and the LCD screen as well as the operating mode. In this project, the screen has the greatest impact on speed, limiting it to the refresh rate by default. This gives a result of 61.5 thousand measurements per second with a single sampling. The actual measuring speed of the device is much higher, but it has not yet been the subject of detailed research. It will be obtained for offline imaging, i.e. collecting measurement data and their subsequent visualization in a higher time resolution on a computer. The presented project can be an important element in complex systems in process tomography [11-26] and optimization solutions [27-37].

Control system

The control system used in the project is a 32-bit STMicroelectronics STM32F429ZIT6 microcontroller located on the STM32F429I-DISC1 development board. It was built based on the high-performance ARM Cortex M4 core, has 2 MB flash memory and 256 KB RAM. The development board is equipped with a 2.4-inch QVGA TFT LCD display. The screen uses the LTDC (LCD TFT Display Controller) and the aforementioned RAM, thanks to which it is possible to achieve high data transfer speeds with a 24-bit color palette.



Fig. 2. Development board STM32F429I-DISC1.

The resistive touch layer of the screen communicates with the microcontroller using the SPI protocol in half-duplex mode. STM32F429I-DISC1 has an integrated ST-LINK / V2 programmer, with which you can quickly program the system. The board is powered by a microUSB socket. STMicroelectronics provides free software: TouchGFX Designer with a library of libraries and TouchGFX extensions for creating graphical interfaces, STM32CubeMX for initial equipment configuration and STM32CubeIDE for creating embedded software, debugging code, compiling it and communicating with the programmer.

The embedded software of the control system operates on the basis of the FreeRTOS real-time system. In separate threads it supports the operation of the control system itself, the LCD screen and operations related to controlling the data acquisition module. This design, based on data queuing, facilitates the management of transmitted results and synchronization of data acquisition with the displayed image.

Data acquisition module

The data acquisition module of the WMS type sensor presented in this work is powered from an external DC source with voltage + 5 V and symmetrical ± 9 V. It can be controlled via any external microprocessor system in the 3 - 5V range logic (in this case 3V from the system STM32F429I-DISC1). The acquisition module includes both a sending and receiving part. The transmission transmits the excitation signal to the working part in the form of a sequence of pulses on individual transmission lines. This signal is fed to the sensor from the outside and switched by the module using analog keys controlled using decoders. The receiving part of the acquisition module detects the set signals and determines their level using an analog-to-digital converter. Then the numerical data is directly processed into an image, where each signal level is assigned the appropriate color of pixels.

WMS sensors are characterized by very high speed of work. The shortest acquisition time is achieved in multi-transducer systems in which each receiving line is connected to a separate analog-to-digital converter. This solution, however, has a major drawback, which is the high cost of the device. Instead of many separate integrated circuits, it was decided to use two 16-channel converters with successive approximation of Analog Devices AD7490. They are equipped with sequencers that automatically change measuring channels. The measurement resolution is 12 bits and the throughput reaches 1 MSPS. They are powered from a single source with a voltage of 2.7-5.25 V. The conversion frequency is regulated by the frequency of the serial transmission clock. This solution ensures full

synchronization of conversion time with the speed of data transfer to the control system. The maximum clock frequency is 20 MHz.

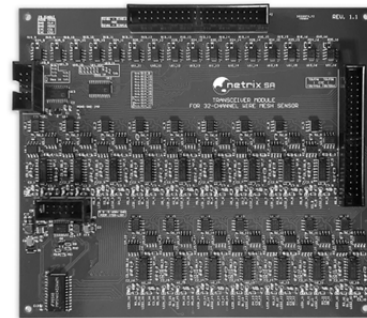


Fig. 3. WMS acquisition module.

The acquisition module is equipped with 4 IDC slots. Two 40-pin are used to connect to the working part of the device, the other two 10-pin to connect an external source of excitation signal, control transducers (SPI), key control (binary) and to connect the power supply of the module itself. The set voltage on the first transmission line is measured successively by all receiving lines. Then it is set to the next one and again measured by all receiving lines. The measuring cycle ends after measuring the signal set on the last transmission line. While voltage is present on one of the transmission lines, the others are shorted to ground. The working part of the sensor is placed at the connection of pipes with the tested medium in such a way that all lines are in the light of the internal diameter of the pipeline. The connection between the working part and the data acquisition module are two 40-pin IDC tapes.

The working part of the sensor

The working part of the sensor is made of 0.08 mm thick, uninsulated, gold-plated molybdenum wires stretched on a dielectric frame. 32 parallel send lines are placed perpendicular to 32 parallel receive lines and are two planes separated by 2.5 mm spacing. Thanks to this, in the absence of flow of the tested medium, they are not physically or electrically connected with each other. The lines on each plane are 2.7 mm apart. The intersection points of the transmitting and receiving lines correspond to the pixels of the received image. The impedance level at these points is represented on the screen of the control device using the appropriate color.

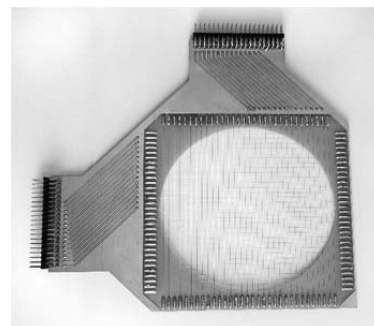


Fig. 4. WMS working part.

The set voltage on the first transmission line is measured successively by all receiving lines. Then it is set to the next one and again measured by all receiving lines. The measuring cycle ends after measuring the signal set on the last transmission line. While voltage is present on one of the transmission lines, the others are shorted to ground.

The working part of the sensor is placed at the connection of pipes with the tested medium in such a way that all lines are in the light of the internal diameter of the pipeline. The connection between the working part and the data acquisition module are two 40-pin IDC tapes.

Construction work

Construction works carried out at the Research and Development Center Netrix S.A. were intended to create a full-size device 32 x 32 lines, i.e. a size not seen in the literature. This posed new challenges for the designer, mainly related to the speed of acquisition and the way of presenting the results. Additionally, due to the large number of sending and receiving channels, the data acquisition module has been designed on a four-layer laminate. The upper and lower layers are used to carry signals. The middle two are digital ground and power lines. The work carried out so far has involved the development of two versions of the working part and two prototypes of the acquisition module. The last prototype is currently in the phase of embedded software optimization and testing. The first prototype of a separate data acquisition module was used to develop the firmware of the ARM STM32 chip controlling the WMS sensor. It was also intended to show preliminary estimates of the quality and pace of work of the entire device. The second prototype contains important structural corrections and crowns the structural part of the research and development process of this project.

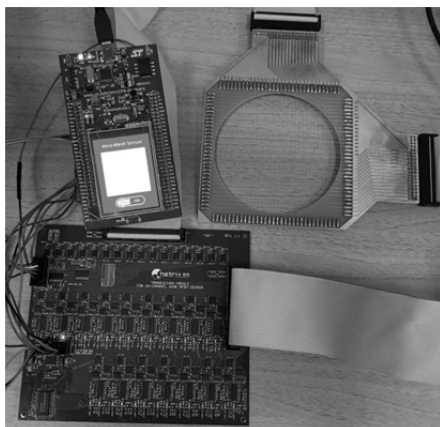


Fig. 5. Complete WMS system: control system, acquisition module and working part.

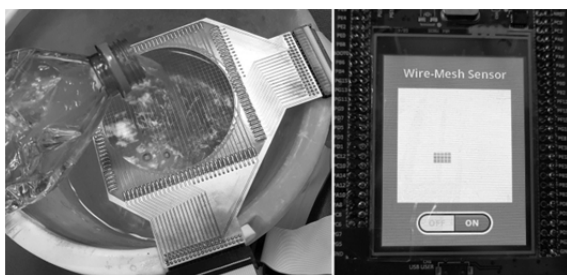


Fig. 6. WMS while working on a prototype stand. On the left water is poured through the sensor, on the right measurement visualization.

It contains a number of changes, which include:

- replacement of analogue-digital converters for many times faster,
- adding passive interference protection in the working part,
- redesigning the power lines to facilitate the analysis of installation problems,

- redesigning the excitation signal line,
- adding a buffer on binary decoder control lines to increase compatibility with different levels of logic signal voltages,
- adding a second buffer on digital data transmission lines in order to improve transmission quality and increase compatibility with various voltage levels of logic signals,
- redesigning measuring amplifier circuits in the receiving section,
- reducing the number of sockets for communication with the control device,
- moving all sockets to the upper part of the system,
- placing full descriptions on the PCB descriptive layer,
- any design changes to achieve the above (adding additional filters, voltage stabilizer, etc.).

The presented set of the most important components has already been tested in previous research and development projects of Netrix S.A. on process tomography as reliable, easy to implement and later use. The device can record measurement results at high speed for later analysis and off-line image analysis. It can also adjust the pace to the refresh rate of the LCD screen with e.g. simultaneous multiple sampling. When using a control system based on the ARM STM32F4 architecture, the estimated off-line imaging speed is above 1000 frames per second with a single sampling.

Other work to be done includes corrections to the embedded control system software and appropriate research on the operation and effectiveness of the device. In addition, the impact of the construction of the working part on the quality of the received images will be determined. Ultimately, the optimally constructed working part will be placed in the multiphase flow test kit.

Conclusion

The article presents the Wire-mesh sensor project. It is a device used for invasive imaging of vertical and horizontal flows of liquids and gases. It does not require any complicated software reconstruction, which is why it is characterized by very high operating speed, which depends to the greatest extent on the conversion time of the analog-to-digital converter used. The sensor consists of two parts: the acquisition module and the working part. The speed of the device depends on the microprocessor system used to control the entire system. The device will be able to record measurement results at high speed for later analysis and analysis of the off-line image. When using the ARM STM32F4 architecture control system, the estimated speed is above 1000 frames per second for a single sample.

Authors: Tomasz Rymarczyk, Ph.D. Eng., University of Economics and Innovation, Projektowa 4, Lublin, Poland/ Research & Development Centre Netrix S.A. E-mail: tomasz@rymarczyk.com; Jakub Szumowski, Research & Development Centre Netrix S.A., E-mail: jakub.szumowski@netrix.com.pl; Tomasz Cieplak Ph.D., Lublin University of Technology, Nadbystrzycka 38A, Lublin, Poland, E-mail: t.cieplak@pollub.pl; Konrad Niderla, University of Economics and Innovation, Projektowa 4, Lublin, Poland/ Research & Development Centre Netrix S.A. E-mail: konrad.niderla@netrix.com.pl; Przemysław Adamkiewicz, Ph.D., University of Economics and Innovation, Projektowa 4, Lublin, Poland/ Research & Development Centre Netrix S.A. E-mail: p.adamkiewicz@netrix.com.pl;

REFERENCES

- [1] Szumowski J., Rymarczyk T., Adamkiewicz P., Wire-mesh sensor for invasive imaging of vertical and horizontal flows of liquids and gases, 2019 Applications of Electromagnetics in Modern Engineering and Medicine, PTZE 2019, 2019, 241-245

- [2] Rodriguez, I., Velasco, H.F., Rodriguez, O.M., & Riano, „Capacitive wire-mesh sensor measurements in oilwater flow”, A.B. (2014).
- [3] Dos Santos E. N., Da Silva M. J., Morales R. E. M., Thiele S., Schleicher E., Hampel U., Novel wire-mesh sensor for the visualization of three-phase flows, 15th Brazilian Congress of Thermal Sciences and Engineering, November 10-13, 2014, Belém, PA, Brazil
- [4] Da Silva M. J., Dos Santos E. N., Hampel U., Rodriguez I. H., Rodriguez O. M. H., Phase fraction distribution measurement of oil–water flow using a capacitance wire-mesh sensor, *Measurement Science and Technology* 22, 2011
- [5] Da Silva M. J., Hampel U., Capacitance wire-mesh sensor applied for the visualization of three-phase gas–liquid–liquid flows, *Flow Measurement and Instrumentation*, 34 (2013), 113–117.
- [6] Sharaf S., Da Silva M., Hampel U., Zippe C., Beyer M., Azzopardi B., Comparison between wire mesh sensor and gamma densitometry void measurements in two-phase flows, *Measurement Science and Technology* 22, 2011
- [7] Da Silva M. J., Schleicher E., Hampel U., Advanced wire-mesh sensor technology for fast flow imaging, IST 2009 - International Workshop on Imaging Systems and Techniques, Shenzhen, China, May 11-12, 2009
- [8] Da Silva M. J., Hampel U., Arruda L., Amaral C. E. F., Morales R., Experimental Investigation of Horizontal Gas-Liquid Slug Flow by Means of Wire-Mesh Sensor, *Journal of the Brazilian Society of Mechanical Sciences and Engineering*, 33 (2010), 234-242.
- [9] Santos E., Reinecke S., Schleicher E., Hampel U., Da Silva M., Wire-mesh sensor applied to solid concentration visualization in slurries, 7th International Symposium on Process Tomography, Dresden, Germany, 1 - 3 September 2015.
- [10] Sujiwa A., Endarko E., Wire-Mesh 16 × 16 Capacitance Sensor for Analysis of Capacitance Distribution on Cylindrical Pipe, The 3rd International Seminar on Science and Technology, August 3rd 2017, Surabaya, Indonesia
- [11] About L., Grudziń K., Wiącek J., Niedostatkiewicz M., Karpiński B., and Szkodo M., Selection of material for X-ray tomography analysis and DEM simulations: comparison between granular materials of biological and non-biological origins, *Granul. Matter*, 20 (2018), No. 3, 38.
- [12] Grudziń K., Romanowski A., Chaniecki Z., Niedostatkiewicz M., Sankowski D., Description of the silo flow and bulk solid pulsation detection using ECT, *Flow Measurement and Instrumentation*, 21 (2010), No. 3, 198-206.
- [13] Kryszyn J., Wanta D. M., Smolik W. T., Gain Adjustment for Signal-to-Noise Ratio Improvement in Electrical Capacitance Tomography System EVT4, *IEEE Sens. J.*, 17 (2017), No. 24, 8107–8116.
- [14] Nowakowski J., Ostalczyk P., Sankowski D., Application of fractional calculus for modelling of two-phase gas/liquid flow system, *Informatyka, Automatyka, Pomiary w Gospodarce i Ochronie Środowiska (IAPGOŚ)*, 7 (2017), No. 1, 42-45.
- [15] Majchrowicz M., Kapusta P., Jackowska-Strumiłło L., Sankowski D., Acceleration of image reconstruction process in the electrical capacitance tomography 3d in heterogeneous, multi-gpu system, *Informatyka, Automatyka, Pomiary w Gospodarce i Ochronie Środowiska (IAPGOŚ)*, 7 (2017), No. 1, 37-41
- [16] Romanowski A., Big Data-Driven Contextual Processing Methods for Electrical Capacitance Tomography, in *IEEE Transactions on Industrial Informatics*, 15 (2019), No. 3, 1609-1618.
- [17] Rymarczyk T., Kłosowski G. Innovative methods of neural reconstruction for tomographic images in maintenance of tank industrial reactors. *Eksploatacja i Niezawodność – Maintenance and Reliability*, 21 (2019); No. 2, 261–267
- [18] Rymarczyk, T.; Kozłowski, E.; Kłosowski, G.; Niderla, K. Logistic Regression for Machine Learning in Process Tomography, *Sensors*, 19 (2019), 3400.
- [19] Kłosowski G., Rymarczyk T., Gola A., Increasing the reliability of flood embankments with neural imaging method. *Applied Sciences*, 8 (2018), No. 9, 1457.
- [20] Rymarczyk T., Adamkiewicz P., Polakowski K., Sikora J., Effective ultrasound and radio tomography imaging algorithm for two-dimensional problems, *Przegląd Elektrotechniczny*, 94 (2018), No 6, 62-69
- [21] Rymarczyk T., Szumowski K., Adamkiewicz P., Tchórzewski P., Sikora J., Moisture Wall Inspection Using Electrical Tomography Measurements, *Przegląd Elektrotechniczny*, 94 (2018), No 94, 97-100
- [22] Duda K., Adamkiewicz P., Rymarczyk T., Niderla K., Nondestructive Method to Examine Brick Wall Dampness, *International Interdisciplinary PhD Workshop Location: Brno, Czech Republic Date: SEP 12-15, 2016*, 68-71
- [23] Smolik W., Kryszyn J., Olszewski T., Szabatin R., Methods of small capacitance measurement in electrical capacitance tomography, *Informatyka, Automatyka, Pomiary w Gospodarce i Ochronie Środowiska (IAPGOŚ)*, 7 (2017), No. 1, 105-110.
- [24] Wajman R., Fiderek P., Fidos H., Sankowski D., Banasiak R., Metrological evaluation of a 3D electrical capacitance tomography measurement system for two-phase flow fraction determination, *Measurement Science and Technology*, 24 (2013), No. 6, 065302.
- [25] Wang M., *Industrial Tomography: Systems and Applications*, Elsevier, 2015.
- [26] Ye Z., Banasiak R., Soleimani M., Planar array 3D electrical capacitance tomography, *Insight: Non-Destructive Testing and Condition Monitoring*, 55 (2013), No. 12, 675-680.
- [27] Dušek J., Hladký D., Mikulka J., Electrical Impedance Tomography Methods and Algorithms Processed with a GPU, In *PIERS Proceedings*, 2017, 1710-1714.
- [28] Goetzke-Pala A., Hoła A., Sadowski Ł., A non-destructive method of the evaluation of the moisture in saline brick walls using artificial neural networks. *Archives of Civil and Mechanical Engineering*, 18 (2018), No 4, 1729-1742.
- [29] Kozłowski E., Mazurkiewicz D., Kowalska B., et al., Binary Linear Programming as a Decision-Making Aid for Water Intake Operators, 1st International Conference on Intelligent Systems in Production Engineering and Maintenance (ISPEM), Wrocław, Poland, Sep 28-29, 2017, Book Series: *Advances in Intelligent Systems and Computing*, 637 (2018), 199-208.
- [30] Krawczyk A., Korzeniewska E., Łada-Tondyrya, E. Magnetophosphenes – History and contemporary implications, *Przegląd Elektrotechniczny*, 94 (2018), No 1, 61-64.
- [31] Korzeniewska E., Gałazka-Czarnecka I., Czarnecki A., Piekarska A., Krawczyk A., Influence of PEF on antocyanins in wine *Przegląd Elektrotechniczny*, 94 (2018), No 1, 57-60.
- [32] Kozłowski E., Mazurkiewicz D., Zabiński T., Prucnal S., Sęp J., Assessment model of cutting tool condition for real-time supervision system, *Eksploatacja i Niezawodność – Maintenance and Reliability*, 21 (2019); No 4, 679–685
- [33] Vališ D., Hasilová K., Forbelská M., Vintř Z., Reliability modelling and analysis of water distribution network based on backpropagation recursive processes with real field data, *Measurement* 149 (2020), 107026
- [34] Kowalska A., Banasiak R., Romanowski A., Sankowski D., Article 3D-Printed Multilayer Sensor Structure for Electrical Capacitance Tomography, 19 (2019), *Sensors*, 3416
- [35] Gocłowski J., Korzeniewska E., Sekulska-Nalewajko J. et al., Extraction of the Polyurethane Layer in Textile Composites for Textronics Applications Using Optical Coherence Tomography, *POLYMERS*, 10 (2018), No. 5, 469
- [36] Gałazka-Czarnecka, I.; Korzeniewska E., Czarnecki A. et al., Evaluation of Quality of Eggs from Hens Kept in Caged and Free-Range Systems Using Traditional Methods and Ultra-Weak Luminescence, *Applied Sciences-Basel*, 9 (2019), No. 12, 2430.
- [37] Valis D., Mazurkiewicz D., Application of selected Levy processes for degradation modelling of long range mine belt using real-time data, *Archives of Civil and Mechanical Engineering*, 18 (2018), No. 4, 1430-1440.